Synergistic Substrate Inhibition of *ent*-Copalyl Diphosphate Synthase: A Potential Feed-Forward Inhibition Mechanism Limiting Gibberellin Metabolism[1][OA]

Sladjana Prisic and Reuben J. Peters*

Department of Biochemistry, Biophysics, and Molecular Biology, Iowa State University, Ames, Iowa 50011

Gibberellins (GAs) or gibberellic acids are ubiquitous diterpenoid phytohormones required for many aspects of plant growth and development, including repression of photosynthetic pigment production (i.e. deetiolation) in the absence of light. The committed step in GA biosynthesis is catalyzed in plastids by *ent*-copalyl diphosphate synthase (CPS), whose substrate, (E,E,)-geranylgeranyl diphosphate (GGPP), is also a direct precursor of carotenoids and the phytol side chain of chlorophyll. Accordingly, during deetiolation, GA production is repressed, whereas flux toward these photosynthetic pigments through their common GGPP precursor is dramatically increased. How this is accomplished has been unclear because no mechanism for regulation of CPS activity has been reported. We present here kinetic analysis of recombinant pseudomature CPS from Arabidopsis (*Arabidopsis thaliana*; rAtCPS) demonstrating that Mg^{2+} and GGPP exert synergistic substrate inhibition effects on CPS activity. These results suggest that GA metabolism may be limited by feed-forward inhibition of CPS; in particular, the effect of Mg^{2+} because light induces increases in plastid Mg^{2+} levels over a similar range as that observed here to affect rAtCPS activity. Notably, this effect is most pronounced in the GA-specific AtCPS because the corresponding activity of the resin acid biosynthetic enzyme abietadiene synthase is 100-fold less sensitive to $[Mg^{2+}]$. Furthermore, Mg^{2+} allosterically activates the plant porphobilinogen synthase involved in chlorophyll production. Hence, Mg^{2+} may have a broad role in regulating plastidial metabolic flux during deetiolation. Finally, the observed synergistic substrate/feed-forward inhibition of CPS also seems to provide a novel example of direct regulation of enzymatic activity in hormone biosynthesis.

GAs are key phytohormones required for many aspects of plant growth and development, including initiation of seed germination and subsequent repression of photosynthetic pigment production in the absence of light (for review, see Fleet and Sun, 2005). Genes in the GA metabolic pathway are quickly upregulated during germination (Yamaguchi et al., 2001) and a high level of GA is maintained until seedlings reach light, which triggers a drop in the level of bioactive GA (Ait-Ali et al., 1999; Gil and Garcia-Martinez, 2000; O'Neill et al., 2000; Reid et al., 2002; Symons and Reid, 2003). This initial drop in active GA levels is needed for deetiolation (i.e. photosynthetic pigment production) because GA represses such photomorphogenesis (Alabadi et al., 2004).

The committed step in GA biosynthesis is catalyzed in plastids by *ent*-copalyl diphosphate synthase (CPS), whose substrate, (*E,E,E*)-geranylgeranyl diphosphate (GGPP), is also a direct precursor of photosynthetic pigments (i.e. carotenoids and the phytol side chain of chlorophyll; Fig. 1). Accordingly, control of CPS activity represents a logical regulatory point. Early studies of GA metabolism suggested that kaurene production, initially thought to be produced from GGPP by a single enzyme, is a key regulatory step in GA biosynthesis (West et al., 1982). It was later discovered that kaurene is formed in two distinct cyclization reactions that are catalyzed by two separate enzymes in plants, a protonation-initiated cyclization reaction catalyzed by CPS followed by a pyrophosphate ionization-initiated cyclization reaction catalyzed by kaurene synthase (KS; Duncan and West, 1981; Fig. 2). CPS gene expression is developmentally controlled and it has been suggested that this is the primary control point regulating CPS activity and, hence, the flow of GGPP into GA biosynthesis (Silverstone et al., 1997; Smith et al., 1998). Overexpression studies have demonstrated that kaurene biosynthesis is limited by CPS and not KS activity (Fleet et al., 2003), further emphasizing the gatekeeping role of CPS.

Because of its critical role in GA biosynthesis, a number of different CPS genes have been identified, including those from Arabidopsis (*Arabidopsis thaliana*), corn (*Zea mays*), pumpkin (*Cucurbita maxima*), pea
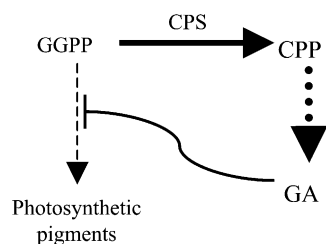
Figure 1. Relationship between GAs and plant pigment production in the dark. GGPP is a common precursor for photosynthetic pigments and GAs. CPS converts GGPP into CPP as the committed step in GA biosynthesis. In the dark, high concentrations of GA inhibit production of pigments from GGPP. Dashed arrows indicate multiple steps in biosynthetic pathways.

(*Pisum sativum*), rice (*Oryza sativa*), and sweet broomweed (*Gutierrez sarothrae*; Sun and Kamiya, 1994; Bensen et al., 1995; Ait-Ali et al., 1997; Smith et al., 1998; Otomo et al., 2004; Prisic et al., 2004; Sakamoto et al., 2004; Xu et al., 2004; Nakagiri et al., 2005). All of the corresponding enzymes contain a DXDD motif in common with the otherwise phylogenetically unrelated, yet mechanistically similar (i.e. protonation-initiated), squalene-hopene cyclases (Wendt et al., 1997) and are founding members of an enzymatic family that has been termed class II diterpene cyclases (Sun and Kamiya, 1994; Wendt and Schulz, 1998). Although phylogenetically related, class I terpene cyclases, such as KS, are mechanistically distinct and contain a different Asp-rich motif (DDXXD) placed on a separate domain (Christianson, 2006; Fig. 2). It has been established from mechanistic studies and crystal structures of several class I enzymes that the associated DDXXD motif is involved in binding divalent metal ions, generally Mg^{2+} (Lesburg et al., 1997; Starks et al., 1997; Rynkiewicz et al., 2001). These divalent metal ions are involved in both binding the pyrophosphate group and catalyzing ionization and, therefore, are required for class I pyrophosphate ionization-initiated catalysis (Christianson, 2006). In contrast, whereas divalent metal ions potently activate class II (i.e. protonation-initiated) cyclization of GGPP, their presence is not absolutely required for this type of cyclization (Peters and Croteau, 2002). Mutations in the class II diterpene cyclase-associated DXDD motif have much greater effects on catalysis than the absence of divalent metal ions (Peters and Croteau, 2002). Thus, it has been hypothesized that the conserved DXDD motif found in class II diterpene cyclases is involved in carbon-carbon double-bond protonation of GGPP, rather than binding divalent metal ions (Peters et al., 2001; Peters and Croteau, 2002). Recently, direct mechanistic evidence for this hypothesis has been obtained (Prisic et al., 2007).

The initial drop of bioactive GA in the response of etiolated seedlings to light has been suggested to arise from down-regulation of the last step in GA biosynthesis, as well as an increase in GA catabolism (Reid et al., 2002). However, to satisfy the high demand for

GGPP in photosynthetic pigment biosynthesis during deetiolation, the 2-C-methyl-D-erythritol-4-P pathway that supplies isoprenoid precursors in plastids is upregulated by light (Carretero-Paulet et al., 2002). Notably, futile flux into GA metabolism seems to be suppressed because only relatively small increases are seen in the level of GA intermediates and catabolites (Reid et al., 2002), although CPS gene transcription is not affected by light (Chang et al., 2005). Whereas it has been reported that CPS is preferentially expressed in nonphotosynthetic cell types (Silverstone et al., 1997) and its enzymatic activity is associated with proplastids and is essentially absent from mature chloroplasts (Aach et al., 1995), presumably due to some level of posttranscriptional regulation during plastid development, no such regulatory mechanism has been reported during deetiolation. It also has been reported that CPS exhibits significant GGPP-dependent substrate inhibition (Frost and West, 1977; Kawaide et al., 2000), which has been suggested to play a role in regulating GA biosynthesis (Kawaide et al., 2000). However, the corresponding mechanism is not well understood nor is it clear how the observed GGPP-dependent substrate inhibition relates to the hypothetical increase in GGPP concentration. Thus, how plants limit GA metabolism, despite the presumed increase in levels of the common GGPP precursor, remains an open question.

Motivated by the importance of CPS in GA metabolism and the existing uncertainties regarding the catalytic mechanism of class II diterpene cyclases more generally, we have undertaken detailed enzymatic analysis of CPS from Arabidopsis (AtCPS; Sun and Kamiya, 1994). To carry out these studies, a pseudomature recombinant version of AtCPS was developed (rAtCPS). Intriguingly, the kinetic properties of rAtCPS seem to be correlated to its physiological role in controlling flux into GA metabolism and suggest a general role for magnesium in coordinating metabolic fluxes in plant plastids during their response to light.

RESULTS

Development of Recombinant Pseudomature rAtCPS

Diterpene synthases are directed to plastids, where diterpene biosynthesis occurs (Croteau et al., 2000) by an N-terminal transit peptide sequence that is removed after import, releasing the mature active
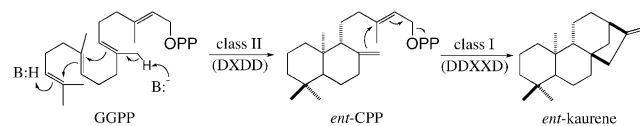
Figure 2. Committed steps in GA biosynthesis. CPS converts GGPP into CPP via a protonation-initiated (i.e. class II) mechanism. Further cyclization of CPP into kaurene is catalyzed by KS, which removes the pyrophosphate group from the substrate, as is characteristic of prototypical (i.e. class I) terpene cyclases.

enzyme (Bohlmann et al., 1998). Inclusion of this transit peptide sequence appears to interfere with soluble recombinant expression of full-length diterpene synthases, as previously reported (Smith et al., 1998; Peters et al., 2000; Williams et al., 2000; Xu et al., 2004). Thus, to carry out the desired biochemical studies, it was necessary to define a functional pseudomature AtCPS construct suitable for recombinant expression.

While the exact N terminus of native AtCPS is not known, plastid import experiments have indicated that the mature enzyme is approximately 10 kD smaller than the full-length protein (Sun and Kamiya, 1994). Further, previous recombinant truncation studies in the context of glutathione-S-transferase fusion proteins indicated the two pumpkin CPSs lost activity if they were truncated beyond a conserved point; 99 and 107 amino acids for CmCPS1 and CmCPS2, respectively (Smith et al., 1998). Hence, we initially constructed and expressed the corresponding truncation of AtCPS (i.e. removal of the initial 100 amino acid residues [Δ100]). This truncation was not well expressed despite trials with several different *Escherichia coli* host strains under a variety of conditions. Hypothesizing that suboptimal codon usage near the N terminus might be negatively affecting recombinant expression (Bulmer, 1988), the first 10 codons of AtCPSΔ100 were optimized for bacterial expression. However, this optimized construct also was not well expressed. To operationally define functional pseudomature constructs, nine additional truncations of AtCPS, corresponding to removal of 33 to 95 amino acids (Δ33, Δ50, Δ63, Δ70, Δ75, Δ80, Δ84, Δ90, and Δ95), were made using the N-terminal rule (Varshavsky, 1996) and exon-splicing sites (Sun and Kamiya, 1994) to guide the choice of truncation sites.

Four of the constructed truncations, Δ50, Δ63, Δ84, and Δ90, appeared to be reasonably well expressed and active, as judged by SDS-PAGE (Fig. 3) and preliminary enzymatic assays with crude extracts. Initial characterization indicated that Δ50 was extremely unstable, whereas the more extensively truncated constructs Δ84 and Δ90 were clearly more stable. Both Δ84 and Δ90 could be purified in a four-step chromatography protocol, resulting in approximately 5 mg/L of bacterial culture of highly pure protein as judged by SDS-PAGE. Preliminary biochemical analysis indicated that AtCPSΔ84 had slightly better enzymatic activity and was somewhat more stable than Δ90. Furthermore, the junction between residues 84 and 85 also corresponds to an exon boundary in the AtCPS gene, representing a logical truncation site. Accordingly, AtCPSΔ84 was chosen for further analysis as a recombinant pseudomature version of AtCPS (rAtCPS).

The truncation study described here may be useful as a general guide for recombinant expression of class II terpene cyclases because their sequences are much more conserved following the later pseudomature truncation points (Δ84 and Δ90) identified with AtCPS. However, this does not necessarily lead to constructs suitable for overexpression. We have made equivalent truncations for other CPS enzymes, such as those we

have previously identified from rice (Prisic et al., 2004; Xu et al., 2004) and maize (Harris et al., 2005) and, although we did see improvements in expression and/or activity, the expression levels did not approach that observed with rAtCPS.

Characterization of rAtCPS

Notably, during SDS-PAGE analysis, rAtCPS appears smaller than its calculated molecular mass, running at approximately 75 kD rather than approximately 84 kD. To verify that the purified protein was intact, electrospray ionization (ESI)-mass spectrometry (MS) was performed, demonstrating the expected 83.8-kD molecular mass. Thus, rAtCPS exhibits abnormally high mobility in SDS-PAGE analysis, consistent with previous observations wherein the full-length protein was estimated to be approximately 86 kD and the native mature enzyme approximately 76 kD by SDS-PAGE analysis (Sun and Kamiya, 1994). This approximately 10-kD difference after in vivo processing is also similar to the 9.2-kD difference between the calculated molecular mass for full-length AtCPS (93 kD) and rAtCPS. Dynamic light-scattering analysis indicated a mass of 86 kD for rAtCPS in solution, indicating that the recombinant protein is monomeric, consistent with previous investigation of native CPS from wild cucumber (*Echinocystis macrocarpa/Marah macrocarpus*; Duncan and West, 1981).

Development of a Kinetic Assay for Class II Diterpene Synthase Activity

rAtCPS stored in the absence of dithiothreitol (DTT) quickly lost enzymatic activity, exhibited a wide irregular pattern of mass additions in ESI-MS analysis, and rapidly precipitated out of solution. This is consistent with early studies on CPS from wild cucumber demonstrating that the native enzyme can be stabilized with DTT (Frost and West, 1977). Hence, it appears that thiol groups are very important for CPS structure and/or activity, which was utilized to develop an
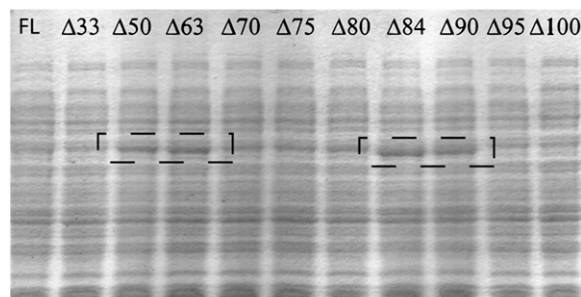
Figure 3. Expression analysis of AtCPS truncation series. SDS-PAGE of recombinant bacterial soluble extracts obtained from OverExpress C41(DE3) clones transformed with plasmids carrying genes for full-length or truncated AtCPS. The four truncations that showed better expression are indicated by the dashed boxes. FL, Full-length AtCPS.

effective assay for kinetic analysis; specifically, use of the thiol-directed alkylating agent *N*-ethylmaleimide (NEM) to terminate enzymatic activity. Following NEM-mediated inactivation of rAtCPS, the substrate and product are dephosphorylated with alkaline phosphatase and analyzed by gas chromatography (GC); initially, GC-MS for product verification, but generally GC-flame ionization detection for quantification. The rates of product formation were measured by calculating the fractional conversion of the known starting substrate concentration to product. Initial time-course studies demonstrated that the catalytic rate is no longer linear after approximately 8% conversion. Reaction rates were linear with enzymatic concentrations down to 12 nM rAtCPS. Unfortunately, it was not possible to use stabilizing proteins, such as bovine serum albumin or lysozyme because they decrease the rate at which NEM alkylation terminates CPS activity. Accordingly, incubation times were varied to achieve 2% to 8% turnover with this minimal 12 nM concentration of rAtCPS, with assays typically being 15 s to 4 min in duration. Finally, rAtCPS exhibits optimal activity between pH 7.5 and 8.0 and kinetic assays were typically performed at pH 7.75.

Magnesium Cofactor Dependence of rAtCPS Activity

Terpene synthases require a divalent metal ion cofactor, most commonly Mg^{2+}, for their enzymatic activity (Christianson, 2006). This requirement extends to the class II diterpene cyclases such as CPS (Frost and West, 1977), although divalent metal ions do not appear to be as critical in these mechanistically distinct enzymes (Peters and Croteau, 2002). Consistent with this latter observation, whereas the calculated $k_{cat} = 3.3 \text{ s}^{-1}$ under optimal conditions (see below), in the absence of a divalent metal ion cofactor (i.e. even after extensive dialysis against 0.1 M EDTA and with 2 mM EDTA present in the assay buffer), rAtCPS still converts GGPP into copalyl diphosphate (CPP) with a calculated $k_{cat} = 0.0043 \text{ s}^{-1}$ (Table I). By contrast, Ala substitution for the middle Asp of the DXDD motif results in an enzyme (rAtCPS:D379A) with a catalytic rate of approximately 10^{-7} s^{-1} even under optimal conditions (Table II). Note that circular dichroism analysis (data not shown) indicates that the rAtCPS:D379A mutant is correctly folded, at least containing equivalent amounts of secondary structure as the wild-type enzyme. These results imply that a divalent metal ion cofactor is not absolutely required for class II catalysis,

which is consistent with previous work on the bifunctional (i.e. class II and class I activity containing) diterpene cyclase abietadiene synthase (Peters and Croteau, 2002). Presumably, the divalent metal ion is required for substrate binding, potentially in a complex with the pyrophosphate moiety of the GGPP substrate (e.g. the dissociation constants for nucleoside diphosphates and Mg^{2+} are 0.2 to 0.7 mM [Dawson et al., 1989]).

The divalent metal ion specificity of rAtCPS was determined through kinetic assays with various metal ions and Mg^{2+} was found to be most effective. Only partial activity was observed with Ni^{2+}, Co^{2+}, Ca^{2+}, and Cu^{2+}, whereas Mn^{2+} and Fe^{2+} appeared to interfere with the assay, although this is most likely due to inhibition of alkaline phosphatase rather than rAtCPS and, thus, it is possible that these ions also may stimulate rAtCPS activity to some extent (Fig. 4).

To determine the optimal concentration of Mg^{2+} for rAtCPS activity, saturation experiments were carried out. Intriguingly, the Mg^{2+} dependence curve was distinctly biphasic, with a sharp maximum around 0.1 mM (Fig. 5A). Treating Mg^{2+} as a cosubstrate, the observed kinetic data were fit to the substrate inhibition equation, yielding similar apparent dissociation constants for activating and inhibitory Mg^{2+} binding, with $K_M^{Mg} = 56 \pm 14 \ \mu M$ and $K_i^{Mg} = 94 \pm 26 \ \mu M$ (Table III).

Magnesium Cofactor Dependence of rAgAS Class II Activity

To test whether this distinct biphasic response to Mg^{2+} is a common feature of class II diterpene cyclases or more specifically restricted to the GA-associated AtCPS, the Mg^{2+} dependence of the class II activity of recombinant abietadiene synthase from grand fir (*Abies grandis*; rAgAS) was examined because AgAS acts in conifer resin acid biosynthesis (i.e. secondary metabolism). To confine the analysis to rAgAS class II activity, the D621A mutant that eliminates the class I activity of this otherwise bifunctional diterpene cyclase was utilized. In particular, rAgAS:D621A will only convert GGPP into CPP (of normal stereochemistry) and does not catalyze its further cyclization to abietadiene, although it contains full class II activity because the effect of D621A is restricted to the class I active site (Peters et al., 2001). Notably, whereas the Mg^{2+} activating binding constant for the class II activity of rAgAS ($K_M^{Mg} = 40 \pm 7 \ \mu M$) was very similar to that for rAtCPS, the inhibitory binding constant was

Table I. *Kinetic parameters of rAtCPS*

$MgCl_2$	k_{cat}	K_M	K_i	k_{cat}/K_M
mM	s^{-1}	μM	μM	
0 (with 2mM EDTA)	0.0043 ± 0.0002	4.2 ± 0.3	47 ± 6	0.001
0.1	3.3 ± 0.6	2.9 ± 0.8	4.7 ± 1.3	1.1
1	1.8 ± 0.5	0.7 ± 0.3	1.1 ± 0.4	2.6
Ratio 0.1:1	1.8	4.1	4.3	0.4

Table II. *Kinetic parameters of rAtCPS:D379A mutant*

$MgCl_2$	k_{cat}	K_M	K_i
mM	*s^{-1}*	*μM*	*μM*
0.1	$(3 \pm 1) \times 10^{-7}$	16 ± 11	–

more than 100 times larger ($K_i^{Mg} = 12 \pm 4$ mM; Table III; Fig. 5B).

Kinetic Analysis of rAtCPS

Substrate inhibition effects from GGPP also have been previously observed with CPS (Frost and West, 1977; Kawaide et al., 2000), as well as for the class II activity of rAgAS (Peters et al., 2000). Notably, the magnitude of the GGPP substrate inhibition effect on rAtCPS activity varied with Mg^{2+} concentration, demonstrating synergism between the inhibitory effects of these two cosubstrates (Fig. 5C). At 1 mM Mg^{2+}, rAtCPS exhibited GGPP-dependent substrate inhibition similar to that previously reported for native CPS from wild cucumber assayed in the presence of 0.5 mM Mg^{2+} (i.e. substrate inhibition is observed at GGPP concentrations higher than 1 μM; Frost and West, 1977). However, at the optimal concentration of 0.1 mM Mg^{2+}, the calculated k_{cat} increases almost 2-fold and both pseudobinding constants, K_M and K_i, also increase around 4-fold (Table I). This results in a nominal decrease in enzymatic efficiency (k_{cat}/K_M) of more than 2-fold. However, the decrease in Mg^{2+} concentration also decreases the substrate inhibition effect of GGPP, resulting in an overall increase in enzymatic activity for GGPP concentrations above 1 μM. Visual inspection of the kinetic plots reveals the potential for an up to 10-fold decrease in CPS activity at higher concentrations of Mg^{2+} and GGPP through their synergistic substrate inhibition effects (Fig. 5C, arrow). In addition, removal of Mg^{2+} significantly reduced substrate inhibition by GGPP (Fig. 5D; Table I), confirming the synergistic effect of Mg^{2+}. Substrate inhibition with GGPP was not observed in experiments with rAtCPS: D379A under optimal conditions, implying that K_i is increased to levels greater than the maximum 20 μM GGPP substrate levels used here, which indicates that this mutation impairs the inhibitory binding site (Table II).

DISCUSSION

Among the several fates for GGPP in plant metabolism, that of GA is the least likely in terms of allocated carbon flux. For example, levels of bioactive GA are ≤ 10 ng/g (Symons and Reid, 2003), whereas carotenoids often comprise ≥ 10 μg/g (Rodriguez-Amaya, 2001) of fresh tissue, representing at least a 1,000-fold difference. Previous reports have demonstrated that the level of bioactive GA is controlled by transcriptional regulation of the 2-oxoglutarate-dependent dioxygenases (GA oxidases) acting to produce (GA 20-oxidase

and GA 3-oxidase) and initiate degradation (GA 2-oxidase) of these phytohormones (for review, see Hedden and Phillips, 2000). The efficiency of this downstream control has been demonstrated through experiments with CPS- and KS-overexpressing Arabidopsis strains, which accumulate kaurene and kaurenoic acid, but not downstream bioactive GA metabolites (Fleet et al., 2003). However, as CPS catalyzes the committed biosynthetic step, flux into GA metabolism must be controlled by regulation of CPS activity. This regulation largely has been studied at the level of gene transcription, which is developmentally controlled (Silverstone et al., 1997; Smith et al., 1998). Nevertheless, the potent bioactivity of GA indicates that multiple layers of control (e.g. enzymatic levels and biochemical activity) may be exerted to limit GA metabolism, particularly during deetiolation with its corresponding large metabolic flux through GGPP toward photosynthetic pigments (i.e. carotenoids and the phytol side chain of chlorophyll), whereas biosynthesis of GA metabolites (bioactive and otherwise) is suppressed.

GA represses photomorphogenesis, including deetiolation; hence, the production of photosynthetic pigment requires decreased levels of bioactive GA (Alabadi et al., 2004). This reduction was suggested to occur solely via suppression of biosynthetic GA 3-oxidase, which catalyzes the last step in bioactive GA production and up-regulation of the catabolic GA 2-oxidase (Reid et al., 2002). However, despite the enormous increase in flux toward photosynthetic pigment production through their common GGPP precursor (Rodriguez-Concepcion et al., 2004), relatively little increase in levels of GA metabolites is observed (Reid et al., 2002). Whereas CPS is preferentially expressed in nonphotosynthetic cell types (Silverstone et al., 1997) and its activity is associated with proplastids and seems to be
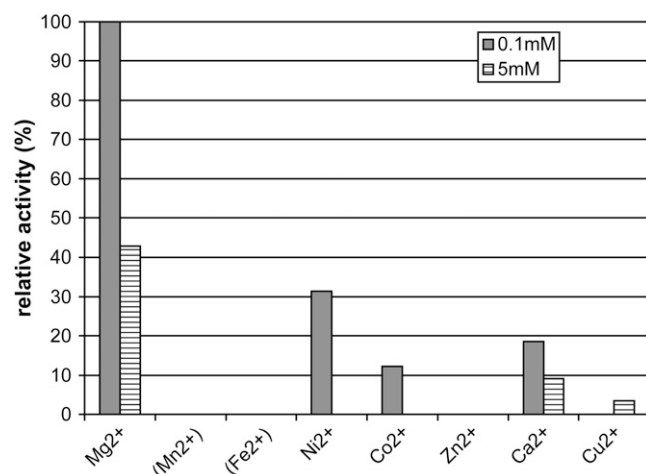
Figure 4. Relative enzymatic activities (% turnover) of rAtCPS in the assays with 0.1 and 5 mM divalent metal ions. Enzymatic activities are normalized to 0.1 mM Mg^{2+} turnover. Mn^{2+} and Fe^{2+} interfered with the assay and therefore their effect on CPS activity could not be determined.

Figure 5. Effect of magnesium on class II diterpene cyclase activity. A, Mg^{2+} dependence of rAtCPS activity. Inset depicts activity over the lower concentration range of Mg^{2+}. B, Mg^{2+} dependence of rAgAS:D621A activity. Saturation experiments shown in A and B were performed with 9 μM GGPP and fit to the substrate inhibition equation, treating Mg^{2+} as a cosubstrate. C, Synergistic effects of Mg^{2+} and GGPP on rAtCPS activity. Squares represent data from a kinetic experiment with 1 mM Mg^{2+} and diamonds are with 0.1 mM Mg^{2+}. Dotted arrow indicates a combined decrease of AtCPS activity with increasing concentrations of GGPP and Mg^{2+}. D, Reduced substrate inhibition effects from GGPP on rAtCPS activity in the presence of 2 mM EDTA. Error bars represent SD from two independent measurements in all cases.
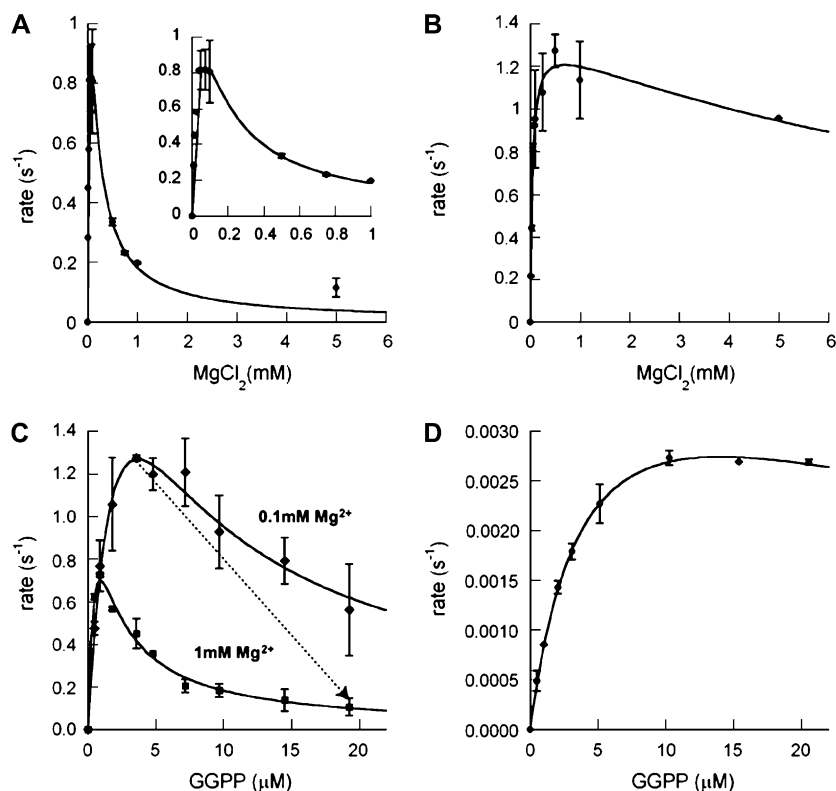

essentially absent from chloroplasts (Aach et al., 1995), indicating transcriptional and posttranscriptional regulation during chloroplast development, we hypothesize that the kinetic properties of CPS reported here represent an additional regulatory mechanism limiting GA metabolism, at least in deetiolation, although potentially also more broadly in chloroplast development. Specifically, it has been demonstrated that light induces an increase in Mg^{2+} levels in plastids (Ishijima et al., 2003), along with up-regulation of the 2-C-methyl-D-erythritol-4-P pathway that provides isoprenoid precursors for the production of GGPP in plastids (Carretero-Paulet et al., 2002; Rodriguez-Concepcion et al., 2004). Whereas the previously noted GGPP-dependent substrate inhibition of CPS has been suggested to regulate GA metabolism (Kawaide et al., 2000), any increase in GGPP levels remains hypothetical given the difficulties inherent in measuring the physiological concentration of this labile metabolite. By contrast, it is particularly notable that the light-induced increase in plastid Mg^{2+} concentration is from submillimolar to millimolar levels (Ishijima et al., 2003), very similar to the range observed here to affect CPS activity (Fig. 5A). Accordingly, we hypothesize that light-induced increases in Mg^{2+} and potentially GGPP may act to limit flux into GA metabolism through the synergistic substrate/feed-forward inhibition effect on CPS activity observed here, while allowing enormous flux toward photosynthetic pigments (Figs. 5C and 6). Consistent with this hypothesis, class II activity of the diterpene cyclase AgAS involved in conifer resin acid

biosynthesis (i.e. secondary metabolism) is significantly less sensitive to Mg^{2+} substrate inhibition effects than the GA biosynthesis-specific AtCPS. However, any such biochemical regulation of CPS enzymatic activity must operate in concert with previously observed transcriptional (Silverstone et al., 1997) and posttranslational (Aach et al., 1995) regulatory mechanisms.

From the biphasic nature of the Mg^{2+}-dependent activity curve (Fig. 5A), there must be at least two distinct divalent metal ion-binding sites in CPS, one that activates its activity and another that inhibits catalysis. Whereas the class II diterpene cyclase DXDD motif represents a potential divalent metal ion-binding site, the 10,000-fold greater loss of activity seen with mutation of the middle Asp to Ala (rAtCPS:D379A; k_{cat} approximately 10^{-7} s^{-1}) relative to simply removing metal ions (k_{cat} approximately 10^{-3} s^{-1}) strongly indicates that these Asps are not involved in binding the activating Mg^{2+}. By analogy to a similar DXDD motif in the otherwise unrelated, yet mechanistically similar (i.e. protonation-initiated) triterpene cyclases, it has been hypothesized that the DXDD Asps in class II diterpene cyclases are similarly involved in protonation (Peters and Croteau, 2002) and direct mechanistic

Table III. *Kinetic parameters for Mg^{2+} saturation*

| Enzyme	k_{cat}	K_M	K_i
	s^{-1}	μM	μM
rAtCPS	2.2 ± 0.4	56 ± 14	94 ± 26
rAgAS:D621A	1.35 ± 0.06	40 ± 7	$12,000 \pm 4,000$
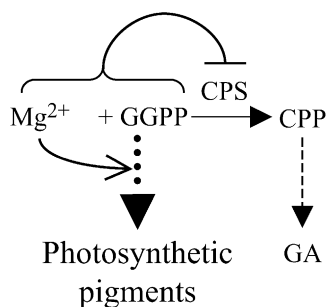
Figure 6. Synergistic substrate/feed-forward inhibition effect of Mg^{2+} and GGPP on CPS activity limits flux into GA metabolism during deetiolation. Also depicted is the activating effect of Mg^{2+} on photosynthetic pigment production (i.e. allosteric activation of plant porphobilinogen synthase). Dashed arrows indicate multiple steps in biosynthetic pathways.

evidence for this hypothesis has recently been obtained (Prisic et al., 2007). Hence, the activating Mg^{2+} must bind elsewhere in the class II active site, presumably to assist proper substrate positioning, potentially in a complex that includes the pyrophosphate moiety of GGPP (Fig. 7A, productive mode). Nevertheless, it also seems likely that the DXDD motif could be involved in binding Mg^{2+}. This would form an unproductive complex that sterically blocks the CPS active site (Fig. 7B; Mg^{2+} inhibition mode). Accordingly, the DXDD motif would then contribute to the observed inhibitory Mg^{2+}-binding site. In addition, it seems likely that this Mg^{2+} would also be able form a complex with the pyrophosphate moiety of GGPP (Fig. 7C, synergistic inhibition mode), consistent with the observed synergistic substrate inhibition (Fig. 5C). Further bolstering this hypothesis, mutations in the DXDD motif of rAtCPS and the class II activity of rAgAS have more significant effects on the observed GGPP inhibitory binding constant, K_i, than the productive pseudobinding constant, K_M (Table II; Peters and Croteau, 2002). Because the observed synergistic substrate inhibition may arise from nonproductive GGPP and/or Mg^{2+} binding in the active site rather than elsewhere, this may be an intrasteric, rather than an allosteric, mediated effect. However, resolution of the exact location of the activating and inhibitory Mg^{2+} binding sites will require structural elucidation of a class II active site.

Our findings further demonstrate that binding of the inhibitory Mg^{2+} in AgAS, a secondary metabolism-specific class II diterpene cyclase, is quantitatively different from that of the GA phytohormone-specific AtCPS (Fig. 5; Table III), yet both contain a DXDD motif. However, due to the trans nature of peptide bonds, only two of the three Asps from the DXDD motif are likely to be able to participate in the hypothesized ligation of an inhibitory Mg^{2+}. Because Mg^{2+} is often coordinated by three protein-derived amino acid ligands (Dudev et al., 1999), there is the potential need for an additional ligand to fully coordinate this divalent

metal ion. Accordingly, the difference in affinity of inhibitory Mg^{2+} binding between AgAS and AtCPS may arise from changes in the nature of this potential ligand (i.e. amino acid Z in Fig. 7) from a residue able to participate in Mg^{2+} binding (e.g. AtCPS) to one unable to do so (e.g. AgAS). This would provide a means by which the observed synergistic substrate inhibition could be utilized to regulate GA phytohormone biosynthesis, while allowing relaxation of this putative feed-forward inhibition mechanism in enzymes involved in secondary metabolism such as AgAS.

In addition to the specific effect of Mg^{2+} on CPS activity demonstrated here, it previously has been shown that Mg^{2+} acts as an allosteric activator of plant porphobilinogen synthase, which is involved in chlorophyll production (Frankenberg et al., 1999; Kervinen et al., 2000; Breinig et al., 2003). Furthermore, the observed effects of Mg^{2+} seem to be characteristic of the plant versions of both CPS and porphobilinogen synthase. It has been reported that a fungal bifunctional CPS/KS does not exhibit substrate inhibition
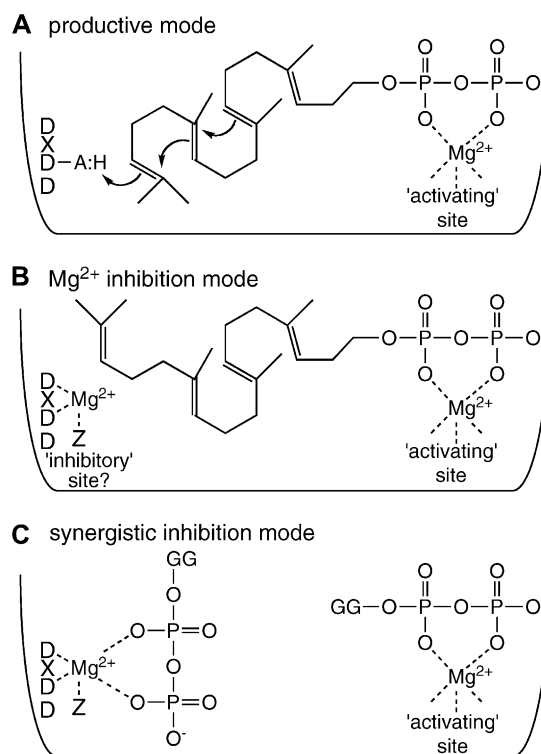
Figure 7. Proposed model for GGPP and Mg^{2+} binding to class II diterpene cyclases. A, Productive binding mode, GGPP-Mg^{2+} complex poised for AtCPS catalyzed cyclization. B, Unproductive Mg^{2+} inhibition mode, binding of Mg^{2+} at the active site interfering with proper binding of GGPP-Mg^{2+} complex. C, Unproductive synergistic substrate inhibition mode, double GGPP-Mg^{2+} complex binding to AtCPS. GG, Geranylgeranyl (either of these hydrocarbon tails may also bind in the hydrophobic portion of the active site). The Z in B and C represents a potential third Mg^{2+} ligand whose presence varies with metabolic function (e.g. is conserved in GA-specific enzymes but not those involved in secondary metabolism).

(Kawaide et al., 2000), and the secondary metabolism-specific AgAS, as well as porphobilinogen synthases from mammals, yeast (*Saccharomyces cerevisiae*), and many bacteria, do not respond to changes in Mg^{2+} concentrations (Jaffe, 2000). Thus, plants may have specifically evolved the ability to use the observed light-induced increase in plastid Mg^{2+} levels, presumably necessary for incorporation of this metal ion into chlorophyll, as a general regulator of metabolic flux during chloroplast development, particularly deetiolation in response to light (Fig. 6).

CONCLUSION

In summary, we have developed a recombinant pseudomature version of AtCPS that enables detailed biochemical analysis. The observed kinetic properties of rAtCPS demonstrate synergistic substrate/feed-forward inhibition of CPS activity by Mg^{2+} and GGPP. We hypothesize that this kinetic behavior may be physiologically relevant, acting to limit GA metabolism, particularly during photosynthetic pigment production in the process of deetiolation. Furthermore, the specific effects of Mg^{2+} on plant enzymes reported here and elsewhere are consistent with a broad role for this divalent metal ion in regulating metabolic flux during deetiolation/chloroplast development. Finally, the observed synergistic substrate/feed-forward inhibition also would represent the first example of direct biochemical (i.e. steric) regulation of enzymatic activity in hormone biosynthesis from any organism.

MATERIALS AND METHODS

Chemicals

The preparation of a reference sample of *ent*-CPP has been previously described (Xu et al., 2007) and was kindly provided by Dr. Robert Coates. Unless otherwise noted, all other chemicals were purchased from Fisher Scientific and molecular biology reagents from Invitrogen.

Cloning of Full-Length and Truncated AtCPS and the rAtCPS:D379A Mutant

The CPS gene from Arabidopsis (*Arabidopsis thaliana*) has previously been cloned (Sun and Kamiya, 1994) and was kindly provided by Dr. Tai-ping Sun. The corresponding open reading frame was transferred into the Gateway vector system via PCR amplification and directional topoisomerase-mediated insertion into pENTR/SD/D-TOPO and verified by complete sequencing. The resulting clone was subsequently transferred via directional recombination to the T7 promoter-based expression vector pDEST14. Truncations were made using primers that amplified the gene from the targeted sites, along with the introduction of an initiating Met codon, cloned into pENTR/SD/D-TOPO, verified by complete sequencing, and transferred to pDEST14 as described in the manufacturer's manual. Site-directed mutagenesis to construct rAtCPS:D379A was carried out via PCR amplification of the pENTR/rAtCPS vector with overlapping mutagenic primers. The resulting mutant gene was verified by complete sequencing and then transferred to pDEST14.

Cloning of Truncated AgAS:D621A

The truncated pseudomature D621A abietadiene synthase mutant from grand fir (*Abies grandis*) that lacks class I activity was kindly provided by Dr.

Rodney Croteau (Peters et al., 2001) and was transferred from pSBET to the Gateway vector system, as described above for the various AtCPS constructs.

Expression and Purification of Recombinant Proteins

Expression studies were carried out with BL21(DE3) (Novagen) and various derivatives (i.e. BL21-AI, BL21star; Novagen), BL21CodonPlus (Stratagene), and OverExpress C41(DE3) (Avidis). OverExpress C41(DE3) gave the best protein yields and was used for all the described studies. Expression was carried out and soluble extract obtained as previously described (Peters et al., 2000). An initial fractionation step was performed with a 100-mL ceramic hydroxyapetite column using a BioLogic LP chromatography system (Bio-Rad). The bound rAtCPS was eluted using a gradient of 10 to 400 mM KH_2PO_4, pH 6.8, over eight column volumes. Further fractionation was carried out with a 50-mL HQ column (Bio-Rad), using a running buffer of 50 mM BisTris, pH 6.8, and eluted with a gradient of 0 to 1 M NaCl over 10 column volumes. The resulting rAtCPS-containing fractions were pooled and desalted on a smaller (6 mL) hydroxyapetite column run as before. Finally, rAtCPS was polished on a 1-mL MonoQ column (Amersham) using an AKTAfplc system with the same buffers used with the HQ column and eluted with a 0 to 1 M NaCl gradient over 20 column volumes. All steps of the purification were carried out at 4°C and rAtCPS was tracked by SDS-PAGE analysis and activity assays. The final protein preparation (approximately 98% pure rAtCPS) was dialyzed against 10 mM BisTris, pH 6.8, 2 mM DTT, 10% glycerol, and stored at 4°C up to 10 d or at −80°C for several months without significant loss in activity. rAgAS:D621A was purified using the same protocol. Notably, after several weeks at 4°C, specific fragmentation of rAtCPS is observed, although this can be prevented by storage in the presence of 5 mM EDTA. rAgAS:D621A does not show such fragmentation and storage with EDTA is not needed. Protein concentrations were determined by A_{280} using the calculated (VectorNTI; Invitrogen) molar extinction coefficients $\varepsilon = 140,860$ M^{-1} cm^{-1} and $\varepsilon = 139,010$ M^{-1} cm^{-1} for rAtCPS and rAgAS, respectively.

Enzymatic Assays

All assays were performed at 30°C in 1 mL of assay buffer (50 mM HEPES, pH 7.75, 100 mM KCl, 10% glycerol) with the indicated divalent metal ion concentration; except for the determination of pH optimum, where pH was varied from pH 6 to 9 in 0.25-unit increments in the presence of 0.1 mM Mg^{2+}. The standard enzyme concentration was 12 nM, except for assays in the absence of any metal and with the rAtCPS:D379A mutant, which required both increased enzyme concentrations and incubation times to detect product formation (e.g. assays with the rAtCPS:D379A mutant were carried out with 4 μM enzyme for 41 h). Activity for the AtCPS truncation series was characterized by simply assaying 100 μL of recombinant bacterial soluble extract, which was incubated with 5 μM GGPP for 15 min at 30°C. Reactions were terminated by adding 100 μL 20 mM NEM in 500 mM Gly, pH 11, then incubating for 5 min at 75°C. Excess NEM was deactivated by adding 20 μL 1 M DTT and incubating for 15 min at room temperature, followed by neutralization with 60 μL 1 M HCl, and the addition of $ZnCl_2$ to 0.1 mM and, if necessary, $MgCl_2$ to 1 mM, before 2 units of bovine alkaline phosphatase (Promega) were added to dephosphorylate both substrate and product, either overnight at room temperature or for 2 h at 37°C. The resulting alcohols (geranylgeraniol and copalol) were extracted three times with 1-mL hexanes, pooled, and concentrated to 25 μL for GC analysis. The stereospecific production of *ent*-CPP was verified by GC-MS detection and comparison with an authentic standard, as previously described (Prisic et al., 2004). After initial product verification, catalytic turnover was quantified by GC-flame ionization detection.

To correct for handling errors, catalytic rates were determined from the observed fractional turnover (i.e. the ratio of product to the sum of product and substrate), along with the known starting concentration of GGPP (Sigma-Aldrich). Kinetic parameters were calculated from fitting the observed data to the substrate inhibition equation (KaleidaGraph 4.0; Synergy Sofware). For all curve fits, $R^2 \geq 0.98$.

For divalent metal ion analysis, 1 mL of purified protein (rAtCPS or rAgAS) was dialyzed twice against 1 L of 0.1 M EDTA, 10% glycerol, 1 mM DTT, 10 mM HEPES, pH 7.4, and then dialyzed against running deionized water for 1 h before it was returned to 1 L of the same buffer without EDTA (all at 4°C for a minimum of 4 h each). The resulting metal-free rAtCPS was preincubated with 0.1 mM or 5 mM $MgCl_2$, $MnCl_2$, $FeSO_4$, $NiSO_4$, $CoCl_2$, $ZnCl_2$, $CaCl_2$, or $CuCl_2$ for 15 min in assay buffer at 30°C before initiating the rAtCPS reaction by the addition of GGPP to 9 μM. For the Mg^{2+} dependence curve

(rAtCPS and rAgAS:D621), MgCl$_2$ was added at various concentrations from 0.01 to 5 mM. To measure activity in the absence of any metal, 2 mM EDTA was included in the assay buffer and the resulting activity compared to that of a control assay with the same metal-free rAtCPS assayed in the presence of 0.1 mM Mg^{2+}.

Biophysical Analysis

Dynamic light scattering was performed on a DynaPro system (Protein Solutions) with 1 mg/mL of rAtCPS in assay buffer. Protein MS analysis was carried out in the Plant Sciences Institute Proteomics facility at Iowa State University with an ABI Q-Star XL quadrupole-time-of-flight tandem mass spectrometer using an ESI source. Circular dichroism was measured using a JASCO J710 spectropolarimeter at room temperature in a cuvette of path length 1 mm. Samples of wild-type and D379A mutant protein were dialyzed against buffer containing 10 mM potassium phosphate, 20% (v/v) glycerol, 5 mM DTT, and 10 mM MgCl$_2$ and diluted to 0.40 mg/mL and 0.41 mg/mL, respectively. Readings were taken in the near-UV spectrum (260–190 nm) and corrected by baseline subtraction.

ACKNOWLEDGMENTS

LITERATURE CITED

Aach H, Bose G, Graebe JE (1995) ent-Kaurene biosynthesis in a cell-free system from wheat (Triticum aestivum L.) seedlings and the localisation of ent-kaurene synthetase in plastids of three species. Planta **197**: 333–342

Ait-Ali T, Frances S, Weller JL, Reid JB, Kendrick RE, Kamiya Y (1999) Regulation of gibberellin 20-oxidase and gibberellin 3β-hydroxylase transcript accumulation during de-etiolation of pea seedlings. Plant Physiol **121**: 783–791

Ait-Ali T, Swain SM, Reid JB, Sun T, Kamiya Y (1997) The LS locus of pea encodes the gibberellin biosynthesis enzyme ent-kaurene synthase A. Plant J **11**: 443–454

Alabadi D, Gil J, Blazquez MA, Garcia-Martinez JL (2004) Gibberellins repress photomorphogenesis in darkness. Plant Physiol **134**: 1050–1057

Bensen RJ, Johal GS, Crane VC, Tossberg JT, Schnable PS, Meeley RB, Briggs SP (1995) Cloning and characterization of the maize An1 gene. Plant Cell **7**: 75–84

Bohlmann J, Meyer-Gauen G, Croteau R (1998) Plant terpenoid synthases: molecular biology and phylogenetic analysis. Proc Natl Acad Sci USA **95**: 4126–4133

Breinig S, Kervinen J, Stith L, Wasson AS, Fairman R, Wlodawer A, Zdanov A, Jaffe EK (2003) Control of tetrapyrrole biosynthesis by alternate quaternary forms of porphobilinogen synthase. Nat Struct Biol **10**: 757–763

Bulmer M (1988) Codon usage and intragenic position. J Theor Biol **133**: 67–71

Carretero-Paulet L, Ahumada I, Cunillera N, Rodriguez-Concepcion M, Ferrer A, Boronat A, Campos N (2002) Expression and molecular analysis of the Arabidopsis DXR gene encoding 1-deoxy-D-xylulose 5-phosphate reductoisomerase, the first committed enzyme of the 2-C-methyl-D-erythritol 4-phosphate pathway. Plant Physiol **129**: 1581–1591

Chang Y-J, Kim B-R, Kim S-U (2005) Metabolic flux analysis of diterpene biosynthesis pathway in rice. Biotechnol Lett **27**: 1375–1380

Christianson DW (2006) Structural biology and chemistry of the terpenoid cyclases. Chem Rev **106**: 3412–3442

Croteau R, Kutchan TM, Lewis NG (2000) Natural products (secondary metabolites). In B Buchanan, W Gruissem, R Jones, eds, Biochemistry and Molecular Biology of Plants. American Society of Plant Biologists, Rockville, MD, pp 1250–1318

Dawson RME, Elliott WH, Jones KM (1989) Data for Biochemical Research. Clarendon Press, Oxford

Dudev T, Cowan JA, Lim C (1999) Competitive binding in magnesium coordination chemistry: water versus ligands of biological interest. J Am Chem Soc **121**: 7665–7673

Duncan JD, West CA (1981) Properties of kaurene synthetase from Marah macrocarpus endosperm: evidence for the participation of separate but interacting enzymes. Plant Physiol **68**: 1128–1134

Fleet CM, Sun T-p (2005) A DELLAcate balance: the role of gibberellin in plant morphogenesis. Curr Opin Plant Biol **8**: 77–85

Fleet CM, Yamaguchi S, Hanada A, Kawaide H, David CJ, Kamiya Y, Sun T-p (2003) Overexpression of AtCPS and AtKS in Arabidopsis confers increased ent-kaurene production but no increase in bioactive gibberellins. Plant Physiol **132**: 830–839

Frankenberg N, Erskine PT, Cooper JB, Shoolingin-Jordan PM, Jahn D, Heinz DW (1999) High resolution crystal structure of a Mg^{2+}-dependent porphobilinogen synthase. J Mol Biol **289**: 591–602

Frost RG, West CA (1977) Properties of kaurene synthase from M. macrocarpus. Plant Physiol **59**: 22–29

Gil J, Garcia-Martinez JL (2000) Light regulation of gibberellin A$_1$ content and expression of genes coding for GA 20-oxidase and GA 3β-hydroxylase in etiolated pea seedlings. Physiol Plant **108**: 223–229

Harris LJ, Saparno A, Johnston A, Prisic S, Xu M, Allard S, Kathiresan A, Ouellet T, Peters RJ (2005) The maize An2 gene is induced by Fusarium attack and encodes an ent-copalyl diphosphate synthase. Plant Mol Biol **59**: 881–894

Hedden P, Phillips AL (2000) Gibberellin metabolism: new insights revealed by the genes. Trends Plant Sci **5**: 523–530

Ishijima S, Uchibori A, Takagi H, Maki R, Ohnishi M (2003) Light-induced increase in free Mg^{2+} concentration in spinach chloroplasts: measurement of free Mg^{2+} by using a fluorescent probe and necessity of stromal alkalinization. Arch Biochem Biophys **412**: 126–132

Jaffe EK (2000) The porphobilinogen synthase family of metalloenzymes. Acta Crystallogr D Biol Crystallogr **56**: 115–128

Kawaide H, Sassa T, Kamiya Y (2000) Functional analysis of the two interacting cyclase domains in ent-kaurene synthase from the fungus Phaeosphaeria sp. L487 and a comparison with cyclases from higher plants. J Biol Chem **275**: 2276–2280

Kervinen J, Dunbrack RL, Litwin S, Martins J, Scarrow RC, Volin M, Yeung AT, Yoon E, Jaffe EK (2000) Porphobilinogen synthase from pea: expression from an artificial gene, kinetic characterization, and novel implications for subunit interactions. Biochemistry **39**: 9018–9029

Lesburg CA, Zhai G, Cane DE, Christianson DW (1997) Crystal structure of pentalene synthase: mechanistic insights on terpenoid cyclization reactions in biology. Science **277**: 1820–1824

Nakagiri T, Lee J-B, Hayashi T (2005) cDNA cloning, functional expression and characterization of ent-copalyl diphosphate synthase from Scoparia dulcis L. Plant Sci **169**: 760–767

O'Neill DP, Ross JJ, Reid JB (2000) Changes in gibberellin A$_1$ levels and response during de-etiolation of pea seedlings. Plant Physiol **124**: 805–812

Otomo K, Kenmoku H, Oikawa H, Konig WA, Toshima H, Mitsuhashi W, Yamane H, Sassa T, Toyomasu T (2004) Biological functions of ent- and syn-copalyl diphosphate synthases in rice: key enzymes for the branch point of gibberellin and phytoalexin biosynthesis. Plant J **39**: 886–893

Peters RJ, Croteau RB (2002) Abietadiene synthase catalysis: conserved residues involved in protonation-initiated cyclization of geranylgeranyl diphosphate to (+)-copalyl diphosphate. Biochemistry **41**: 1836–1842

Peters RJ, Flory JE, Jetter R, Ravn MM, Lee H-J, Coates RM, Croteau RB (2000) Abietadiene synthase from grand fir (Abies grandis): characterization and mechanism of action of the "pseudomature" recombinant enzyme. Biochemistry **39**: 15592–15602

Peters RJ, Ravn MM, Coates RM, Croteau RB (2001) Bifunctional abietadiene synthase: free diffusive transfer of the (+)-copalyl diphosphate intermediate between two distinct active sites. J Am Chem Soc **123**: 8974–8978

Prisic S, Xu J, Coates RM, Peters RJ (2007) Probing the role of the DXDD motif in class II diterpene cyclases. ChemBioChem (in press)

Prisic S, Xu M, Wilderman PR, Peters RJ (2004) Rice contains disparate ent-copalyl diphosphate synthases with distinct metabolic functions. Plant Physiol **136**: 4228–4236

Reid JB, Botwright NA, Smith JJ, O'Neill DP, Kerckhoffs LHJ (2002) Control of gibberellin levels and gene expression during de-etiolation in pea. Plant Physiol **128**: 734–741

Rodriguez-Amaya DB (2001) A Guide to Carotenoid Analysis in Foods. ILSI Press, Washington, DC

Rodriguez-Concepcion M, Fores O, Martinez-Garcia JF, Gonzalez V, Phillips MA, Ferrer A, Boronat A (2004) Distinct light-mediated pathways regulate the biosynthesis and exchange of isoprenoid precursors during Arabidopsis seedling development. Plant Cell 16: 144–156

Rynkiewicz MJ, Cane DE, Christianson DW (2001) Structure of trichodiene synthase from *Fusarium sporotrichioides* provides mechanistic inferences on the terpene cyclization cascade. Proc Natl Acad Sci USA 98: 13543–13548

Sakamoto T, Miura K, Itoh H, Tatsumi T, Ueguchi-Tanaka M, Ishiyama K, Kobayashi M, Agrawal GK, Takeda S, Abe K, et al (2004) An overview of gibberellin metabolism enzyme genes and their related mutants in rice. Plant Physiol 134: 1642–1653

Silverstone AL, Chang C-W, Krol E, Sun T-P (1997) Developmental regulation of the gibberellin biosynthetic gene GA1 in Arabidopsis thaliana. Plant J 12: 9–19

Smith MW, Yamaguchi S, Ait-Ali T, Kamiya Y (1998) The first step of gibberellin biosynthesis in pumpkin is catalyzed by at least two copalyl diphosphate synthases encoded by differentially regulated genes. Plant Physiol 118: 1411–1419

Starks CM, Back K, Chappell J, Noel JP (1997) Structural basis for cyclic terpene biosynthesis by tobacco 5-epi-aristolochene synthase. Science 277: 1815–1820

Sun T-P, Kamiya Y (1994) The Arabidopsis GA1 locus encodes the cyclase *ent*-kaurene synthetase A of gibberellin biosynthesis. Plant Cell 6: 1509–1518

Symons G, Reid J (2003) Hormone levels and response during de-etiolation in pea. Planta 216: 422–431

Varshavsky A (1996) The N-end rule: functions, mysteries, uses. Proc Natl Acad Sci USA 93: 12142–12149

Wendt KU, Poralla K, Schulz GE (1997) Structure and function of a squalene cyclase. Science 277: 1811–1815

Wendt KU, Schulz GE (1998) Isoprenoid biosynthesis: manifold chemistry catalyzed by similar enzymes. Structure 6: 127–133

West CA, Shen-Miller J, Railton ID (1982) Regulation of kaurene synthetase. *In* PF Wareing, ed, Plant Growth Substances. Academic Press, London, pp 81–90

Williams DC, Wildung MR, Jin AQ, Dalal D, Oliver JS, Coates RM, Croteau R (2000) Heterologous expression and characterization of a ''pseudomature'' form of taxadiene synthase involved in paclitaxel (taxol) biosynthesis, and evaluation of a potential intermediate and inhibitors of the multistep diterpene cyclization reaction. Arch Biochem Biophys 379: 137–146

Xu M, Hillwig ML, Prisic S, Coates RM, Peters RJ (2004) Functional identification of rice *syn*-copalyl diphosphate synthase and its role in initiating biosynthesis of diterpenoid phytoalexin/allelopathic natural products. Plant J 39: 309–318

Xu M, Wilderman PR, Morrone D, Xu J, Roy A, Margis-Pinheiro M, Upadhyaya N, Coates RM, Peters RJ (2007) Functional characterization of the rice kaurene synthase-like gene family. Phytochemistry 68: 312–326

Yamaguchi S, Kamiya Y, Sun T-p (2001) Distinct cell-specific expression patterns of early and late gibberellin biosynthetic genes during Arabidopsis seed germination. Plant J 28: 443–453